

The finite-size quantum Ising ring revisited: Real space versus momentum space

Ning Wu^{1,*}

¹*Center for Quantum Technology Research, School of Physics,
Beijing Institute of Technology, Beijing 100081, China*

As perhaps the most studied paradigm for a quantum phase transition, the periodic quantum Ising chain is exactly soluble via the Jordan-Wigner transformation followed by a Fourier transform that diagonalizes the model in the momentum space of spinless fermions. Although the above procedures are well-known, there remain some subtle points to be clarified regarding the correspondence between the real-space and momentum-space representations of the *finite-size* quantum Ising ring, especially those related to fermion parities. In this work, we establish the relationship between the two fully aligned ferromagnetic states in real space and the two degenerate momentum-space ground states of the classical Ising ring, with the former being a special case of the factorized ground states of the more general XYZ model on the frustration-free hypersurface. Based on this observation, we then provide a Pfaffian formula for calculating real-time dynamics of the parity-breaking longitudinal magnetization with the system initially prepared in one of the two ferromagnetic states and under translationally invariant driving. The formalism is shown to be applicable to *large* systems with the help of free online programs for the numerical computation of the Pfaffian, thus providing an efficient method to numerically study, for example, the emergence of time crystals in this model.

I. INTRODUCTION

The one-dimensional quantum Ising model with periodic boundary conditions (or a quantum Ising ring) is usually regarded as one of the two prototypical models for understanding quantum phase transitions [1]. Due to its exact solvability the model has been a testbed for a wide variety of physical phenomena including quantum entanglement in quantum critical phenomena [2–5], quantum quench across a quantum critical point [6–10], dynamical quantum phase transitions [11, 12], and more recently proposed time crystals [13], and so on.

It is well known that the quantum Ising ring can be solved by first performing the Jordan-Wigner transformations that convert the spin operators into spinless fermions, followed by a Fourier transform which maps the fermion model into a free fermion model in the momentum space [14]. The presence of the boundary term connecting the last site of the spin chain to the first one does not lead to a simple cyclic structure in the Jordan-Wigner fermion representation and the full Hilbert space is divided into two subspaces containing even and odd numbers of fermions, respectively. Although for large enough systems one can neglect the boundary corrections in the discussion of quantum phase transitions, it is both interesting and important to study the case of *finite-size* systems in which the boundary terms and the resultant fermion parity effects cannot be neglected [15–17, 19, 20]. For example, it is shown by different approaches that the true ground state of a finite-size quantum Ising ring with even number of sites lies in the subspace with even number of fermions [17, 19, 20].

It is also known that the quantum Ising chain with open boundaries can be mapped into Kitaev's p -wave

superconductor chain with equal pairing and hopping strength [21–23], which can be viewed as a special case of the correspondence between the more general open XYZ spin chain [24] and the interacting Kitaev model [25]. For the open XYZ chain, there exists a frustration-free hypersurface in the parameter space on which the ground state is twofold degenerate and admits separable forms in the spin representation [24]. Due to the equivalence between the XYZ chain and the interacting Kitaev chain with open boundaries, similar twofold separable fermionic ground states occur on the frustration-free line [25]. In general, the above two separable fermion ground states are neither orthogonal to each other nor have definite fermion parity. Nevertheless, simple equally-weighted linear superpositions of the two yields two orthogonal states with distinct fermion parities [25]. It was further shown in [26] that the aforementioned two orthogonal states, one of which having odd fermion parity and the other having even parity, are also the ground states of the interacting Kitaev chain under periodic and antiperiodic boundary conditions, respectively.

Recently, nonequilibrium dynamics of a quantum Ising chain initialized in one of the two fully aligned ferromagnetic states has been considered. In Ref. [12], the dynamics of the nearest-neighbor equal-time longitudinal correlation function under a quench starting with the ferromagnetic state is calculated and shown to exhibit nonanalytic signature that indicates a dynamical critical point. Ref. [13] proposed a simple scheme to generate a discrete time crystal by periodically kick a quantum Ising chain with its initial state prepared in one of the two ferromagnetic states. There, the time evolution of the longitudinal magnetization was numerically calculated using exact diagonalization for relatively small systems.

In this work, we show that the two momentum-space degenerate ground states of the periodic classical Ising model, which are of the BCS form and hence separable, are actually equivalent to the two equally-weighted linear

*Electronic address: wun1985@gmail.com

superpositions of the two ferromagnetic states in the spin representation. This correspondence is shown to be the special case of the XYZ chain under the frustration-free condition. Based on this observation and assuming that the system is prepared in one of the two ferromagnetic states, we are able to obtain the time-evolved state in the momentum space under *translationally invariant driving*. Similar to the initial state, the time-evolved state is also a linear combination of two states with distinct fermion parities. This makes the calculation of expectation values of *parity-breaking* observables such as the longitudinal magnetization subtle due to the mixing of the two parity components. Nevertheless, by writing the BCS-type time-evolved mode states as the occupation of two effective (time-dependent) Bogoliubov fermions, we are able to derive a Pfaffian formula for the expectation value of the longitudinal magnetization. With the help of free online algorithms that can achieve efficient numerical computation of the Pfaffian, the dynamics of the longitudinal magnetization can be probed for large systems and at long-time scales. As two examples, we perform numerical simulations for sudden quenches and periodic delta kicks.

The rest of the paper is structured as follows. In Sec. II, we introduce the Hamiltonian of the quantum Ising ring and describe its diagonalization in detail. In Sec. III we identify the global ground state of the system and establish the relationship between the ferromagnetic states and the momentum-state BCS states of the classical Ising model. In Sec. IV we derive the Pfaffian formula for the dynamics of the longitudinal magnetization and discuss its application to the sudden quench and delta kicks. Conclusions are drawn in Sec. V.

II. MODEL AND DIAGONALIZATION

For the sake of completeness and to introduce the notations that will be used later, we provide in this section the details of the diagonalization of the quantum Ising ring.

A. The BdG form

The one-dimensional ferromagnetic quantum Ising model with N sites is described by the Hamiltonian

$$H_{\text{QIM}} = - \sum_{j=1}^N (\sigma_j^x \sigma_{j+1}^x + g \sigma_j^z), \quad (1)$$

where σ_j^α ($\alpha = x, y, z$) are the Pauli matrices on site j , $g \geq 0$ is the transverse field along the z -direction, and we have set the nearest-neighboring exchange interaction to unit for simplicity. We consider *even* N and impose periodic boundary conditions, i.e., $\vec{\sigma}_{N+1} = \vec{\sigma}_1$.

To diagonalize H_{QIM} , we first perform the Jordan-Wigner transformation [14]

$$\sigma_j^+ \equiv (\sigma_j^x + i\sigma_j^y)/2 = c_j^\dagger T_j, \quad \sigma_j^z = 2c_j^\dagger c_j - 1, \quad (2)$$

where c_j^\dagger creates a spinless fermion on site j , and T_j is the Jordan-Wigner string

$$T_j = e^{i\pi \sum_{l=1}^{j-1} c_l^\dagger c_l}. \quad (3)$$

Note that $T_{N+1} = e^{i\pi \sum_{l=1}^N c_l^\dagger c_l}$ is the fermion parity operator and it can be checked that T_{N+1} is a conserved quantity with eigenvalues ± 1 . The Jordan-Wigner transformation maps the spin model H_{QIM} into a spinless fermion model

$$\begin{aligned} H_F = & - \sum_{j=1}^{N-1} (c_j^\dagger c_{j+1} + c_{j+1}^\dagger c_j + c_j^\dagger c_{j+1}^\dagger + c_{j+1} c_j) \\ & + (c_N^\dagger c_1 + c_1^\dagger c_N + c_N^\dagger c_1^\dagger + c_1 c_N) T_{N+1} \\ & - 2g \sum_{j=1}^N c_j^\dagger c_j + gN, \end{aligned} \quad (4)$$

where we have separated out the bulk and boundary contributions of the hopping and pairing terms.

Since T_{N+1} is conserved and squares to 1, we can separately diagonalize H_F in the two subspaces with even ($T_{N+1} = 1$) and odd ($T_{N+1} = -1$) fermion parity. In turn, we can define two projection operators $P_+ = (1+T_{N+1})/2$ and $P_- = (1-T_{N+1})/2$, which project onto subspaces with even or odd number of fermions, respectively. Using the relation $P_+ + P_- = 1$, the fermion annihilation operator c_j can be written as

$$\begin{aligned} c_j &= (P_+ + P_-) c_j (P_+ + P_-) \\ &= P_+ c_j P_- + P_- c_j P_+. \end{aligned} \quad (5)$$

Typical quadratic terms can be expressed as

$$\begin{aligned} c_i^\dagger c_j &= P_+ c_i^\dagger c_j P_+ + P_- c_i^\dagger c_j P_-, \\ c_i^\dagger c_j^\dagger &= P_+ c_i^\dagger c_j^\dagger P_+ + P_- c_i^\dagger c_j^\dagger P_-. \end{aligned} \quad (6)$$

Using the above equations and note that $T_{N+1} = P_+ - P_-$ and $P_+ P_- = P_- P_+ = 0$, the fermionic Hamiltonian H_F can be rewritten as

$$H_F = \sum_{\sigma=\pm} P_\sigma H_{F,\sigma} P_\sigma, \quad (7)$$

where

$$\begin{aligned} H_{F,\sigma} = & - \sum_{j=1}^{N-1} (c_j^\dagger c_{j+1} + c_{j+1}^\dagger c_j + c_j^\dagger c_{j+1}^\dagger + c_{j+1} c_j) \\ & + \sigma (c_N^\dagger c_1 + c_1^\dagger c_N + c_N^\dagger c_1^\dagger + c_1 c_N) \\ & - 2g \sum_{j=1}^N c_j^\dagger c_j + gN. \end{aligned} \quad (8)$$

We can diagonalize $H_{F,+}$ and $H_{F,-}$ separately since the two subspace are orthogonal to each other. To proceed, we focus on the σ -subspace and define

$$c_{N+1} \equiv -\sigma c_1 \quad (9)$$

then the boundary term in $H_{F,\sigma}$ can be absorbed into the bulk term to form a compact expression

$$H_{F,\sigma} = -\sum_{j=1}^N [(c_j^\dagger c_{j+1} + c_j^\dagger c_{j+1}^\dagger + \text{H.c.}) + 2gc_j^\dagger c_j] + gN. \quad (10)$$

Note that the spatial index j in the sum now runs from 1 to N , which suggests us to introduce the following Fourier transforms

$$c_j = \frac{e^{i\pi/4}}{\sqrt{N}} \sum_{k \in K_\sigma} e^{ikj} c_{k\sigma}, \quad c_{k\sigma} = \frac{e^{-i\pi/4}}{\sqrt{N}} \sum_{j=1}^N e^{-ikj} c_j, \quad (11)$$

where $\{c_{k\sigma}\}$ are the fermion modes in the Fourier space and a factor of $e^{i\pi/4}$ is introduced for later convenience. From Eq. (9), the allowed wave numbers for $\sigma = +$ and $-$ survive in the sets

$$K_+ = \left\{ \frac{(2n+1)\pi}{N} | n = -\frac{N}{2}, -\frac{N}{2} + 1, \dots, \frac{N}{2} - 1 \right\}, \quad (12)$$

and

$$K_- = \left\{ \frac{2n\pi}{N} | n = -\frac{N}{2}, -\frac{N}{2} + 1, \dots, \frac{N}{2} - 1 \right\}, \quad (13)$$

respectively. It is easy to check from Eqs. (11), (12) and (13) that the Fourier modes in the σ -subspace satisfy the usual anticommutation relations

$$\{c_{k\sigma}, c_{k'\sigma}\} = 0, \quad \{c_{k\sigma}, c_{k'\sigma}^\dagger\} = \delta_{kk'}. \quad (14)$$

However, for two wave numbers k and k' from two distinct sets, we have, for example (define $\bar{\sigma} = -\sigma$)

$$\{c_{k\sigma}, c_{k'\bar{\sigma}}^\dagger\} = \frac{1}{N} \sum_{j=1}^N e^{-i(k-k')j} = \frac{2}{N} \frac{1}{e^{i(k-k')} - 1} \quad (15)$$

Such kind of commutation relations can be safely avoided provided we concentrate on each subspace separately. However, as we will see in Sec. IV, they will play an important role in the calculation of the time evolution of the longitudinal magnetization. From Eq. (15), the vacuum expectation value of $c_{k\sigma} c_{k'\bar{\sigma}}^\dagger$ is simply

$$f_{kk'} \equiv \langle 0 | c_{k\sigma} c_{k'\bar{\sigma}}^\dagger | 0 \rangle = \frac{2}{N} \frac{1}{e^{i(k-k')} - 1}. \quad (16)$$

We now insert Eq. (11) into Eq. (10) and note that $\frac{1}{N} \sum_{j=1}^N e^{i(k-k')j} = \delta_{k,k'}$ holds for $k, k' \in K_\sigma$, then straightforward calculation gives

$$H_{F,+} = \sum_{k>0, k \in K_+} H_{k+}, \quad (17)$$

$$H_{F,-} = \sum_{k>0, k \in K_-} H_{k-} + \frac{1}{2}(H_{-\pi,-} + H_{0,-}), \quad (18)$$

where

$$H_{k,\sigma} \equiv -2(c_{k\sigma}^\dagger, c_{-k,\sigma}) \begin{pmatrix} \cos k + g & \sin k \\ \sin k & -\cos k - g \end{pmatrix} \begin{pmatrix} c_{k\sigma} \\ c_{-k,\sigma}^\dagger \end{pmatrix}. \quad (19)$$

Note that $H_{k,-}$ is also well-defined for $k = -\pi$ and 0, for which we have

$$H_{-\pi,-} = 2(1-g)(2c_{-\pi,-}^\dagger c_{-\pi,-} - 1), \quad (20)$$

and

$$H_{0,-} = -2(1+g)(2c_{0,-}^\dagger c_{0,-} - 1). \quad (21)$$

Now, the diagonalization of H_{QIM} is equivalent to diagonalizing each of the mode Hamiltonians, $\{H_{k,\sigma}\}$.

B. Normal modes: $k \neq -\pi$ and $k \neq 0$

For $k \neq -\pi$ and 0, there always exists an *opposite* and *distinct* element $-k$ for each $k > 0$ in both the even and odd subspaces. The even subspace for mode k (do not be confused with the global even space defined by $\sigma = +1$) is spanned by $\{|0\rangle_{k,\sigma}, |k, -k\rangle_\sigma = c_{k,\sigma}^\dagger c_{-k,\sigma}^\dagger |0\rangle_{k,\sigma}\}$, where $|0\rangle_{k,\sigma}$ is the common vacuum of $c_{\pm k,\sigma}$. It is easy to check that in this two-dimensional subspace $H_{k,\sigma}$ has the matrix form

$$\mathcal{H}_{k,\sigma}^{(e)} = 2 \begin{pmatrix} \cos k + g & -\sin k \\ -\sin k & -\cos k - g \end{pmatrix}. \quad (22)$$

Similarly, the odd subspace for mode k is spanned by $\{|-k\rangle_\sigma = c_{-k,\sigma}^\dagger |0\rangle_{k,\sigma}, |k\rangle_\sigma = c_{k,\sigma}^\dagger |0\rangle_{k,\sigma}\}$, it turns out that for $k \neq -\pi$ and 0 we always have

$$\mathcal{H}_{k,\sigma}^{(o)} = \begin{pmatrix} 0 & 0 \\ 0 & 0 \end{pmatrix}. \quad (23)$$

In other words, $|-k\rangle_\sigma$ and $|k\rangle_\sigma$ are two degenerate eigenstates of $H_{k,\sigma}$ with zero-eigenvalue.

The eigenenergies of the ground state and excited state of $\mathcal{H}_{k,\sigma}^{(e)}$ are

$$E_{k\sigma}^{(\text{gs})} = -\Lambda_k, \quad E_{k\sigma}^{(\text{ex})} = \Lambda_k, \quad \Lambda_k = 2\sqrt{g^2 + 2g \cos k + 1}. \quad (24)$$

The corresponding ground and excited states read

$$|G^{(\text{gs})}\rangle_\sigma = \cos \frac{\theta_k}{2} |0\rangle_{k,\sigma} + \sin \frac{\theta_k}{2} |k, -k\rangle_{k,\sigma}, \quad (25)$$

$$|G_k^{(\text{ex})}\rangle_\sigma = \sin \frac{\theta_k}{2} |0\rangle_{k,\sigma} - \cos \frac{\theta_k}{2} |k, -k\rangle_{k,\sigma}, \quad (26)$$

where

$$\begin{aligned} \sin \frac{\theta_k}{2} &= \frac{2 \sin k}{\sqrt{(2 \sin k)^2 + (\Lambda_k - 2 \cos k - 2g)^2}}, \\ \cos \frac{\theta_k}{2} &= \frac{\Lambda_k - 2 \cos k - 2g}{\sqrt{(2 \sin k)^2 + (\Lambda_k - 2 \cos k - 2g)^2}}. \end{aligned} \quad (27)$$

It is useful to note that $\Lambda_k > 0$ for all the normal modes and the lowest two excitation energies (i.e. Λ_k) are achieved for

$$k_e^{(1)} = \pi - \frac{\pi}{N}, \quad k_e^{(2)} = \pi - \frac{3\pi}{N}, \quad (\sigma = +1), \quad (28)$$

$$k_o^{(1)} = \pi - \frac{2\pi}{N}, \quad k_o^{(2)} = \pi - \frac{4\pi}{N}, \quad (\sigma = -1). \quad (29)$$

We see that the ground state for a *normal mode* k is just $|G_k^{(\text{gs})}\rangle$, which is an *even* state. We thus conclude that *the ground state for any normal mode k is always even*.

In summary, the mode Hamiltonian $H_{k,\sigma}$ has four eigenvalues (in decreasing order)

$$\Lambda_k, 0, 0, -\Lambda_k,$$

and the corresponding eigenvectors are

$$|G_k^{(\text{ex})}\rangle_\sigma, |k\rangle_\sigma, |-k\rangle_\sigma, |G_k^{(\text{gs})}\rangle_\sigma,$$

with fermion parities

$$\text{even, odd, odd, even.}$$

It is worth mentioning that for the classical Ising model with $g = 0$, the dispersion becomes a constant $\Lambda_k = 2$. From Eq. (27) we have

$$\begin{aligned} \sin \frac{\theta_k|_{g=0}}{2} &= \frac{\sin k}{\sqrt{(\sin k)^2 + (1 - \cos k)^2}}, \\ \cos \frac{\theta_k|_{g=0}}{2} &= \frac{1 - \cos k}{\sqrt{(\sin k)^2 + (1 - \cos k)^2}}. \end{aligned}$$

Note that for normal modes satisfying $0 < k < \pi$, we always have $\sin \frac{k}{2} > 0$, so that $\sqrt{(\sin k)^2 + (1 - \cos k)^2} = \sqrt{2 - 2 \cos k} = 2 \sin \frac{k}{2}$, giving

$$\begin{aligned} \sin \frac{\theta_k|_{g=0}}{2} &= \cos \frac{k}{2}, \\ \cos \frac{\theta_k|_{g=0}}{2} &= \sin \frac{k}{2}. \end{aligned} \quad (30)$$

C. Special modes in the odd space

Special attention must be paid to $k = -\pi$ and 0, for which neither $|k, -k\rangle$ (it vanishes) nor $\{|-k\rangle, |k\rangle\}$ (the two are the same) is well defined. In fact, from Eqs. (20) and (21) we see that $H_{-\pi,-}$ and $H_{0,-}$ can be written in the basis $\{|0\rangle_{-\pi,-}, |k = -\pi\rangle = c_{-\pi,-}^\dagger |0\rangle_{-\pi,-}\}$ and $\{|0\rangle_{0,-}, |k = 0\rangle = c_{0,-}^\dagger |0\rangle_{0,-}\}$ as

$$\mathcal{H}_{-\pi,-} = \begin{pmatrix} -2(1-g) & 0 \\ 0 & 2(1-g) \end{pmatrix}, \quad (31)$$

and

$$\mathcal{H}_{0,-} = \begin{pmatrix} 2(1+g) & 0 \\ 0 & -2(1+g) \end{pmatrix}, \quad (32)$$

which are already in the diagonal form.

III. GROUND STATE

A. Sub-ground states in the two sectors

Since all the modes in K_+ are normal modes, so the sub ground state (SGS) in the even subspace is always

$$|G_+\rangle = \prod_{k>0, k \in K_+} |G_k^{(\text{gs})}\rangle_+. \quad (33)$$

The corresponding SGS energy is

$$E_{G,+} = - \sum_{k>0, k \in K_+} \Lambda_k. \quad (34)$$

The first excited state in the even space might be obtained by either exciting a single mode q from its ground state $|G_q^{(\text{gs})}\rangle_+$ to its (even) excited state $|G_q^{(\text{ex})}\rangle_+$ (with eigenenergy $+\Lambda_q$), or by exciting two modes q_1 and q_2 to their (odd) excited states $|\pm q_1\rangle_+$ and $|\pm q_2\rangle_+$ (with zero eigenenergy). The minimal energy cost for the former case is $2\Lambda_{k_e^{(1)}}$, while for the latter case is $\Lambda_{k_e^{(1)}} + \Lambda_{k_e^{(2)}} > 2\Lambda_{k_e^{(1)}}$. Therefore, the first excited state in the even subspace is

$$|\text{ex}_+\rangle = |G_{k_e^{(1)}}^{(\text{ex})}\rangle_+ \prod_{k>0, k \in K_+, k \neq k_e^{(1)}} |G_k^{(\text{gs})}\rangle_+, \quad (35)$$

with eigenenergy

$$E_{\text{ex},+} = E_{G,+} + 2\Lambda_{k_e^{(1)}}. \quad (36)$$

Since $\Lambda_{k_e^{(1)}}$ is always positive for finite N , Eq. (36) tells us that *the SGS in the even subspace is nondegenerate*.

The situation in the odd subspace is a little subtle due to the appearance of the special modes $k = -\pi$ and $k = 0$. We define $|\phi_e\rangle$ ($|\phi_o\rangle$) to be the lowest-energy

state with even (odd) fermion parity and *made up of the normal modes* in the odd sector. It is apparent that

$$\begin{aligned} |\phi_e\rangle &= \prod_{k>0, k \in K_-} |G_k^{gs}\rangle_-, \\ |\phi_o\rangle &= |\pm k_o^{(1)}\rangle_- \prod_{k>0, k \in K_-, k \neq k_o^{(1)}} |G_k^{gs}\rangle_-, \end{aligned} \quad (37)$$

which possess energies

$$\begin{aligned} \mathcal{E}_e &= - \sum_{k>0, k \in K_-} \Lambda_k, \\ \mathcal{E}_o &= \mathcal{E}_e + \Lambda_{k_o^{(1)}}. \end{aligned} \quad (38)$$

Given $|\phi_e\rangle$ and $|\phi_o\rangle$, there are four possible ways to construct a physical eigenstate in the odd subspace

$$\begin{aligned} |\psi_1\rangle &= |0\rangle_{-\pi, -} |0\rangle_{0, -} |\phi_o\rangle, \\ |\psi_2\rangle &= |0\rangle_{-\pi, -} |k=0\rangle |\phi_e\rangle, \\ |\psi_3\rangle &= |k=\pi\rangle |k=0\rangle |\phi_o\rangle, \\ |\psi_4\rangle &= |k=\pi\rangle |0\rangle_{0, -} |\phi_e\rangle. \end{aligned}$$

with the corresponding eigenenergies

$$\begin{aligned} E_1 &= 2g + \mathcal{E}_o, \\ E_2 &= -2 + \mathcal{E}_e, \\ E_3 &= -2g + \mathcal{E}_o, \\ E_4 &= 2 + \mathcal{E}_e. \end{aligned}$$

Since $g \geq 0$, the SGS should be either $|\psi_2\rangle$ or $|\psi_3\rangle$. The energy difference between the two states is

$$E_2 - E_3 = 2(g - 1) - 2\sqrt{g^2 - 2g \cos \frac{2\pi}{N}} + 1.$$

For $0 \leq g \leq 1$, it is obvious that $E_2 - E_3 < 0$; for $g > 1$, $E_2 - E_3$ is non-positive as $0 \leq \cos \frac{2\pi}{N} < 1$ for $N \geq 4$. Thus, the SGS in the odd sector must be $|\psi_2\rangle$ for all $g \geq 0$, i.e.

$$|G_-\rangle = |k=0\rangle \prod_{k>0, k \in K_-} |G_k^{(gs)}\rangle_-. \quad (39)$$

The corresponding SGS energy is

$$E_{G,-} = - \sum_{k>0, k \in K_-} \Lambda_k - 2. \quad (40)$$

B. An inequality on the upper unit semicircle: The global ground state

We start this subsection by stating the following elementary mathematical problem: Let P be a point on the positive x -axis and set $OP = x$. The upper half of the unit circle is divided into N (N is even) equal

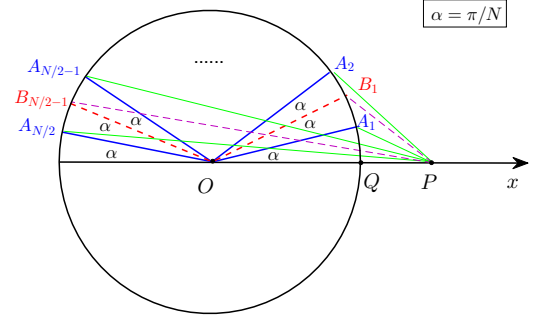


FIG. 1: The upper unit semicircle is divided into N equal sectors, so that $\angle POA_j = (2j - 1)\pi/N$ ($j = 1, 2, \dots, N/2$) and $\angle POB_j = 2j\pi/N$ ($j = 1, 2, \dots, N/2 - 1$).

sectors with angle $\alpha \equiv \pi/N$, such that $\angle POA_j = (2j - 1)\pi/N$ ($j = 1, 2, \dots, N/2$) and $\angle POB_j = 2j\pi/N$ ($j = 1, 2, \dots, N/2 - 1$) (see Fig. 1). Connecting P to each point A_j, B_j , then the following inequality holds:

$$\Delta l(P) \equiv \sum_{j=1}^{N/2} PA_j - \sum_{j=1}^{N/2-1} PB_j \geq 1. \quad (41)$$

It is obvious that the equality holds for $P = O$. Another special point is $P = Q = (1, 0)$, for which we have $QA_j = 2 \sin(j - 1/2)\alpha$ and $QB_j = 2 \sin j\alpha$, then it is easy to show

$$\Delta l(Q) = 1 + \tan \frac{\pi}{4L} > 1. \quad (42)$$

We can straightforwardly prove inequality (41) for $OP = x \geq 1$ by writing $\Delta l(P)$ as

$$\Delta l(P) = \sum_{j=1}^{N/2} f_{2j-1}(x) - \sum_{j=1}^{N/2-1} f_{2j}(x), \quad (43)$$

where $f_j(x) \equiv \sqrt{x^2 - 2x \cos(j\alpha) + 1}$. By noting that $f_N(x) = x + 1$, Eq. (43) can be rewritten as

$$\begin{aligned} \Delta l(P) &= \sum_{j=1}^{N/2} [f_{2j-1}(x) - f_{2j}(x)] + x + 1 \\ &= 2x \sum_{j=1}^{N/2} \frac{\cos 2j\alpha - \cos(2j-1)\alpha}{f_{2j-1}(x) + f_{2j}(x)} + x + 1. \end{aligned} \quad (44)$$

We now observe that $\{f_j(x)\}$ are all monotonically increasing on $[\cos \alpha, +\infty)$ and $\cos 2j\alpha < \cos(2j-1)\alpha$ for all j , which implies that $\Delta l(P)$ is also monotonically increasing on $[\cos \alpha, +\infty)$. By combining this fact with Eq. (42), we thus have

$$\Delta l(P) > \Delta l(Q) > 1, \text{ for } OP > 1, \quad (45)$$

which proves the inequality for $x \geq 1$.

However, the situation is intricate in the region $0 < x < 1$ (i.e., P inside the unit circle) where $\Delta l(P) - 1$

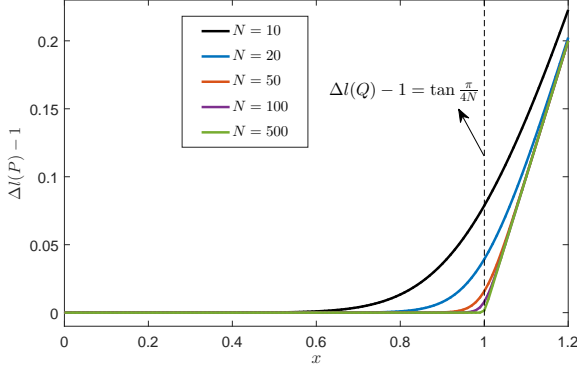


FIG. 2: The quantity $\Delta l(P) - 1$ [see Eq. (41)] as a function of $OP = x$ for various site numbers N .

becomes exponentially small. Though there is evidence that $\Delta l(P) - 1 > 0$ also holds for $0 < x < 1$ (see Fig. 2), a direct proof of this is not obvious since $f_j(x)$ is generally nonmonotonic on $[0, \cos \alpha]$.

To identify the true ground state in the fermionic representation, we have to compare $E_{G,+}$ and $E_{G,-}$. We define the energy difference between the two SGSs

$$\begin{aligned} \Delta(g) &\equiv \frac{1}{2}(E_{G,-} - E_{G,+}) \\ &= \frac{1}{2} \left(\sum_{k>0, k \in K_+} \Lambda_k - \sum_{k>0, k \in K_-} \Lambda_k - 2 \right) \\ &= \sum_{j=1}^{N/2} \sqrt{g^2 + 2g \cos \frac{(2j-1)\pi}{N}} + 1 \\ &\quad - \sum_{j=1}^{N/2-1} \sqrt{g^2 + 2g \cos \frac{2j\pi}{N}} + 1. \end{aligned} \quad (46)$$

Then the ground state will have an even (odd) fermion parity if $\Delta(g) > 0$ (< 0). The function $\Delta(g)$ has the following properties:

i)

$$\Delta(0) = 0, \quad (47)$$

which means that the two SGSs $|G_+\rangle_{g=0}$ and $|G_-\rangle_{g=0}$ are actually degenerate in the absence of the magnetic field. We can also see this in the spin representation, where H_{QIM} reduces to the classical Ising model that has two degenerate ferromagnetic states aligned along the $\pm x$ directions.

ii)

$$\Delta(g) = \Delta(-g), \quad (48)$$

saying that $\Delta(g)$ is an even function. Using this property and comparing Eq. (43) with Eq. (46), we immediately have

$$\Delta(x) = \Delta l(P) - 1. \quad (49)$$

Therefore, the proof of inequality (41) is equivalent to proving $\Delta(g) \geq 0$ for $g \geq 0$, i.e., the true ground state $|\psi_G\rangle$ of H_{QIM} is actually the even SGS $|G_+\rangle$.

Fortunately, $|\psi_G\rangle$ can be directly identified in the spin representation by invoking the Perron-Frobenius theorem [17, 18]. Using the basis in which σ_j^x is diagonalized, i.e., $|\rightarrow\rangle_j = (|\uparrow\rangle_j + |\downarrow\rangle_j)/\sqrt{2}$, $|\leftarrow\rangle_j = (|\uparrow\rangle_j - |\downarrow\rangle_j)/\sqrt{2}$, all of the off-diagonal elements of H_{QIM} are nonpositive and satisfy the connectivity condition (note that $\sigma_j^z |\rightarrow/\leftarrow\rangle_j = |\leftarrow/\rightarrow\rangle_j$). According to the Perron-Frobenius theorem, the ground state of H_{QIM} is nondegenerate and has the form

$$|\psi_G\rangle = \sum_{\alpha_1, \dots, \alpha_N = \rightarrow, \leftarrow} C_{\alpha_1, \dots, \alpha_N} |\alpha_1\rangle_1 \cdots |\alpha_N\rangle_N \quad (50)$$

where the coefficients $C_{\alpha_1, \dots, \alpha_N}$ are strictly positive for any $(\alpha_1, \dots, \alpha_N)$. Due to the \mathbb{Z}_2 symmetry of H_{QIM} under $\sigma_j^x \rightarrow -\sigma_j^x$, the coefficients $C_{\alpha_1, \dots, \alpha_N}$ also satisfy

$$C_{\alpha_1, \dots, \alpha_N} = C_{-\alpha_1, \dots, -\alpha_N}. \quad (51)$$

Combining Eq. (50) with Eq. (51), it is easy to see that $|\psi_G\rangle$ is an even (odd) state for even (odd) N . Thus, H_{QIM} has a unique ground state with even fermion parity for $N = \text{even}$. Furthermore, we have shown that the SGS $|G_+\rangle$ in the even subspace is gapped, so we must have

$$|\psi_G\rangle = |G_+\rangle. \quad (52)$$

We thus proved the inequality given by (41) for $0 < g < 1$ by combining the Perron-Frobenius theorem in matrix theory with the fermion representation of H_{QIM} , which can be viewed as a kind of “physical mathematics” in some sense. We would like to mention that in Refs. [19, 20] a closed-form expression for the energy gap $\Delta(g)$ is provided in the form of an integration.

C. $g = 0$: Separable ground states

For $g = 0$, the quantum Ising model H_{QIM} reduces to the classical Ising model $H_{\text{CIM}} = -\sum_{j=1}^N \sigma_j^x \sigma_{j+1}^x$, which possess two degenerate ground states

$$|\psi_{g=0}^{(r)}\rangle = |\rightarrow\rangle_1 \cdots |\rightarrow\rangle_N, \quad (53)$$

$$|\psi_{g=0}^{(l)}\rangle = |\leftarrow\rangle_1 \cdots |\leftarrow\rangle_N, \quad (54)$$

where $|\rightarrow\rangle_j$ ($|\leftarrow\rangle_j$) denotes the state with the j th spin pointing along the $+x$ ($-x$) direction.

We now have two ways to look at the twofold ground states:

i) In the momentum space, from Eq. (33) and Eq. (39), the two ground states have even and odd fermion parities respectively:

$$|G_+\rangle_{g=0} = \prod_{k>0, k \in K_+} \left(\sin \frac{k}{2} + \cos \frac{k}{2} c_{k,+}^\dagger c_{-k,+}^\dagger \right) |0\rangle_{k,+}, \quad (55)$$

$$|G_{-}\rangle_{g=0} = |k=0\rangle \prod_{k>0, k \in K_{-}} \left(\sin \frac{k}{2} + \cos \frac{k}{2} c_{k,-}^{\dagger} c_{-k,-}^{\dagger} \right) |0\rangle_{k,-}, e^{i\theta+} |G_{+}\rangle_{g=0}, \text{ yielding} \quad (56)$$

$$\left(\frac{1}{\sqrt{2}} \right)^{N-1} = e^{i\theta+} \prod_{k>0, k \in K_{+}} \sin \frac{k}{2} \quad (62)$$

where we have used Eq. (30).

ii) In the real space, the two states $|\psi_{g=0}^{(r/l)}\rangle$ can be written in terms of the Jordan-Wigner fermions as

$$|\psi_{g=0}^{(r/l)}\rangle = \left(\frac{1}{\sqrt{2}} \right)^N \prod_{j=1}^N (1 \pm c_j^{\dagger}) |0\rangle, \quad (57)$$

where $|0\rangle$ is the common vacuum of all $\{c_j\}$. However, neither $|\psi_{g=0}^{(r)}\rangle$ nor $|\psi_{g=0}^{(l)}\rangle$ has a definite fermion parity, as can be seen from the expansion

$$|\psi_{g=0}^{(r/l)}\rangle = \left(\frac{1}{\sqrt{2}} \right)^N \sum_{n=0}^{N/2} \sum_{j_1 < j_2 < \dots < j_{2n}} c_{j_1}^{\dagger} c_{j_2}^{\dagger} \dots c_{j_{2n}}^{\dagger} |0\rangle \\ \pm \left(\frac{1}{\sqrt{2}} \right)^N \sum_{n=1}^{N/2} \sum_{j_1 < j_2 < \dots < j_{2n-1}} c_{j_1}^{\dagger} c_{j_2}^{\dagger} \dots c_{j_{2n-1}}^{\dagger} |0\rangle. \quad (58)$$

We now consider the following two cat states which are equal-weighted superpositions of $|\psi_{g=0}^{(r)}\rangle$ and $|\psi_{g=0}^{(l)}\rangle$

$$|\text{cat}_{+}\rangle = \frac{1}{\sqrt{2}} (|\psi_{g=0}^{(r)}\rangle + |\psi_{g=0}^{(l)}\rangle) \\ = \left(\frac{1}{\sqrt{2}} \right)^{N-1} \sum_{n=0}^{N/2} \sum_{j_1 < j_2 < \dots < j_{2n}} c_{j_1}^{\dagger} c_{j_2}^{\dagger} \dots c_{j_{2n}}^{\dagger} |0\rangle, \quad (59)$$

and

$$|\text{cat}_{-}\rangle = \frac{1}{\sqrt{2}} (|\psi_{g=0}^{(r)}\rangle - |\psi_{g=0}^{(l)}\rangle) \\ = \left(\frac{1}{\sqrt{2}} \right)^{N-1} \sum_{n=1}^{N/2} \sum_{j_1 < j_2 < \dots < j_{2n-1}} c_{j_1}^{\dagger} c_{j_2}^{\dagger} \dots c_{j_{2n-1}}^{\dagger} |0\rangle. \quad (60)$$

It is easy to see that $|\text{cat}_{+}\rangle$ ($|\text{cat}_{-}\rangle$) is a simultaneous eigenstate of T_{N+1} and H_{CIM} , with eigenvalues $+1$ (-1) and $-N$, respectively.

On the other hand, there is a finite energy gap of value 4 between the first excited state and the ground-state manifold of H_{CIM} . Thus, the real-space states $|\text{cat}_{\pm}\rangle$ are expected to be equivalent to the momentum-space states $|G_{\pm}\rangle_{g=0}$, i.e.,

$$|\text{cat}_{\pm}\rangle = e^{i\theta_{\pm}} |G_{\pm}\rangle_{g=0}, \quad (61)$$

where $e^{i\theta_{\pm}}$ are two proportional constants that need to be determined. To this end, we first compare the coefficients of the vacuum state on both sides of $|\text{cat}_{+}\rangle =$

Using the identity $\omega^N + 1 = \prod_{j=1}^N (\omega - e^{i\pi \frac{2j-1}{N}})$, it is easy to show that

$$\prod_{k>0, k \in K_{+}} \sin \frac{k}{2} = \prod_{j=1}^{N/2} \sin \frac{(2j-1)\pi}{2N} \\ = \sqrt{\frac{1}{2^N} \prod_{j=1}^{N/2} |1 - e^{i\pi \frac{2j-1}{N}}|} = \left(\frac{1}{\sqrt{2}} \right)^{N-1},$$

which gives $e^{i\theta+} = 1$, and hence

$$|\text{cat}_{+}\rangle = |G_{+}\rangle_{g=0}. \quad (63)$$

Similarly, by comparing the coefficients of the single-particle component of $|\text{cat}_{+}\rangle = e^{i\theta+} |G_{+}\rangle_{g=0}$, we have $e^{i\theta-} = e^{-i\pi/4}$, giving

$$|\text{cat}_{-}\rangle = e^{-i\pi/4} |G_{-}\rangle_{g=0}. \quad (64)$$

It is worth mentioning that Eq. (64) was explicitly proved in Ref. [23] by transforming the momentum-space state $|G_{-}\rangle_{g=0}$ into the *real space* and showing the consistency of the corresponding coefficients between $|\text{cat}_{-}\rangle$ and the transformed $|G_{-}\rangle_{g=0}$ with the help of mathematical induction. However, our ‘proof’ of Eqs. (63) and (64) is based on physical considerations and is more concise.

Actually, $g = 0$ is a special factorization point of the XYZ model at which the two spatially factorized ground states are *orthogonal* to each other. Consider the XYZ spin chain with open boundary conditions

$$H_{\text{XYZ}}^{(\text{OBC})} = \frac{1}{4} \sum_{j=1}^{N-1} (J_x \sigma_j^x \sigma_{j+1}^x + J_y \sigma_j^y \sigma_{j+1}^y + J_z \sigma_j^z \sigma_{j+1}^z) \\ - \frac{1}{2} \sum_{j=1}^N h_j \sigma_j^z, \quad (65)$$

where we assume $J_x, J_y \leq 0$ and $J_z, h_j \geq 0$, and the inhomogeneous magnetic fields are chosen as $h_1 = h_N = h/2$ and $h_2 = h_3 = \dots = h_{N-1} = h$. We also assume $J_x \neq J_y$ for simplicity. It is known that $[24, 25]$ $H_{\text{XYZ}}^{(\text{OBC})}$ possesses two degenerate spatially separable ground states on the frustration-free hypersurface

$$h = h^* = \sqrt{(J_z - J_x)(J_z - J_y)}. \quad (66)$$

The two ground states are of the form

$$|\Psi^{(\pm)}\rangle = \frac{1}{(1 + \cot \frac{\theta^*}{2})^{N/2}} \\ \left(|\downarrow\rangle_1 \pm \sqrt{\cot \frac{\theta^*}{2}} |\uparrow\rangle_1 \right) \dots \left(|\downarrow\rangle_N \pm \sqrt{\cot \frac{\theta^*}{2}} |\uparrow\rangle_N \right) |0\rangle, \quad (67)$$

where

$$\cot \frac{\theta^*}{2} = \frac{-(J_x - J_y)}{\sqrt{(J_x - J_y)^2 + 4h^{*2} - 2h^*}}. \quad (68)$$

It is important to note that

$$\langle \Psi^{(+)} | \Psi^{(-)} \rangle = \langle \Psi^{(-)} | \Psi^{(+)} \rangle = \left(\frac{1 - \cot \frac{\theta^*}{2}}{1 + \cot \frac{\theta^*}{2}} \right)^N \quad (69)$$

which means $|\Psi^{(+)}\rangle$ and $|\Psi^{(-)}\rangle$ are nonorthogonal unless $\cot \frac{\theta^*}{2} = 1$, or $h^*(J_x - J_y) = 0$. This gives the condition

$$h^* = 0 \quad (70)$$

provided $J_x \neq J_y$. Since we already assumed $J_y, J_x \leq 0$ and $J_z \geq 0$, it is easy to see from Eq. (66) that the only possibilities are $J_z = J_x = 0$ or $J_z = J_y = 0$, for which $H_{XYZ}^{(\text{OBC})}$ reduces to the classical ferromagnetic Ising chain.

The equally-weighted superpositions of $|\Psi^{(+)}\rangle$ and $|\Psi^{(-)}\rangle$ form two orthogonal ground states with distinct fermion parities

$$\begin{aligned} |\tilde{\Psi}^{(e)}\rangle &= \frac{1}{\sqrt{2}}(|\Psi^{(+)}\rangle + |\Psi^{(-)}\rangle), \\ |\tilde{\Psi}^{(o)}\rangle &= \frac{1}{\sqrt{2}}(|\Psi^{(+)}\rangle - |\Psi^{(-)}\rangle). \end{aligned} \quad (71)$$

It was shown in Ref. [26] that $|\tilde{\Psi}^{(e)}\rangle$ ($|\tilde{\Psi}^{(o)}\rangle$) is exactly the ground state of the homogeneous *periodic* XYZ chain

$$\begin{aligned} H_{XYZ}^{(\text{PBC})} &= \frac{1}{4} \sum_{j=1}^N (J_x \sigma_j^x \sigma_{j+1}^x + J_y \sigma_j^y \sigma_{j+1}^y + J_z \sigma_j^z \sigma_{j+1}^z) \\ &\quad - \frac{h}{2} \sum_{j=1}^N \sigma_j^z, \end{aligned} \quad (72)$$

in the subspace with even (odd) numbers of fermions after the Jordan-Wigner transformation.

In the case of $J_x = -4$, $J_y = J_z = 0$ and $h = 2g$, the Hamiltonian $H_{XYZ}^{(\text{PBC})}$ reduces to the Hamiltonian of the quantum Ising ring given by Eq. (1). From Eqs. (66) and (68), we have $h^* = 0$ and $\cot \frac{\theta^*}{2} = 1$, so that the two states $|\Psi^{(\pm)}\rangle$ reduce to $|\psi_{g=0}^{(r/l)}\rangle$ given by Eq. (57).

IV. TIME EVOLUTION FROM $|\psi_{g=0}^{(r)}\rangle$ UNDER TRANSLATIONALLY INVARIANT DRIVING

A. General formalism

In this section, we are interested in the calculation of the dynamics of the longitudinal magnetizations $M_x = \sum_i \sigma_i^x$ and $M_y = \sum_i \sigma_i^y$ when the system is prepared in the ferromagnetic state $|\psi_{g=0}^{(r)}\rangle$ and the driving Hamiltonian is translationally invariant.

From Eqs. (59), (60), (63), and (64), we can write $|\psi_{g=0}^{(r)}\rangle$ as

$$\begin{aligned} |\psi_{g=0}^{(r)}\rangle &= \frac{1}{\sqrt{2}}(|G_+\rangle_{g=0} + e^{-i\frac{\pi}{4}}|G_-\rangle_{g=0}) \\ &= \frac{1}{\sqrt{2}}[\prod_{k>0, k \in K_+} (\sin \frac{k}{2} + \cos \frac{k}{2} c_{k,+}^\dagger c_{-k,+}^\dagger) |0\rangle_{k+} \\ &\quad + e^{-i\frac{\pi}{4}} |k=0\rangle \\ &\quad + \prod_{k>0, k \in K_-} (\sin \frac{k}{2} + \cos \frac{k}{2} c_{k,-}^\dagger c_{-k,-}^\dagger) |0\rangle_{k-}]. \end{aligned} \quad (73)$$

We assume the (possibly time-dependent) driving Hamiltonian $H^{(\text{driv})}(t)$ is translationally invariant so that can be written in the momentum space as

$$\begin{aligned} H^{(\text{driv})} &= \sum_{\sigma=\pm} P_\sigma H_\sigma^{(\text{driv})} P_\sigma, \\ H_+^{(\text{driv})} &= \sum_{k>0, k \in K_+} H_{k,+}^{(\text{driv})}, \\ H_-^{(\text{driv})} &= \sum_{k>0, k \in K_-} H_{k,-}^{(\text{driv})} + \frac{1}{2}(H_{-\pi,-}^{(\text{driv})} + H_{0,-}^{(\text{driv})}) \end{aligned} \quad (74)$$

For most of cases of interest, the representations of $H_{-\pi,-}^{(\text{driv})}$ ($H_{0,-}^{(\text{driv})}$) in the basis $\{|0\rangle_{-\pi,-}, c_{-\pi,-}^\dagger |0\rangle_{-\pi,-}\}$ ($\{|0\rangle_{0,-}, c_{0,-}^\dagger |0\rangle_{0,-}\}$) are diagonal:

$$\begin{aligned} \mathcal{H}_{-\pi,-}^{(\text{driv})} &= \begin{pmatrix} h_1^{(-\pi)}(t) & 0 \\ 0 & h_2^{(-\pi)}(t) \end{pmatrix}, \\ \mathcal{H}_{0,-}^{(\text{driv})} &= \begin{pmatrix} h_1^{(0)}(t) & 0 \\ 0 & h_2^{(0)}(t) \end{pmatrix}. \end{aligned} \quad (76)$$

The time-evolved state is therefore of the form

$$\begin{aligned} |\psi^{(r)}(t)\rangle &= \frac{1}{\sqrt{2}}[\prod_{k>0, k \in K_+} (u_k^{(+)}(t) + v_k^{(+)}(t) c_{k,+}^\dagger c_{-k,+}^\dagger) |0\rangle_{k+} \\ &\quad + e^{-\frac{i}{2} \int_0^t ds [h_1^{(-\pi)}(s) + h_2^{(0)}(s)]} e^{-i\frac{\pi}{4}} \\ &\quad + \prod_{k>0, k \in K_-} (u_k^{(-)}(t) + v_k^{(-)}(t) c_{k,-}^\dagger c_{-k,-}^\dagger) |0\rangle_{k-}] \end{aligned} \quad (77)$$

where the time-dependent coefficients $u_k^{(\pm)}(t)$ and $v_k^{(\pm)}(t)$ satisfy the Schrödinger equation

$$i \begin{pmatrix} \dot{u}_k^{(\pm)} \\ \dot{v}_k^{(\pm)} \end{pmatrix} = \mathcal{H}_{k,\pm}^{(\text{driv})}(t) \begin{pmatrix} u_k^{(\pm)} \\ v_k^{(\pm)} \end{pmatrix} \quad (78)$$

with $\mathcal{H}_{k,\pm}^{(\text{driv})}(t)$ the representations of $H_{k,\pm}^{(\text{driv})}(t)$ in the basis $\{|0\rangle_{k,\pm}, c_{k,\pm}^\dagger c_{-k,\pm}^\dagger |0\rangle_{k,\pm}\}$, and the initial conditions read

$$\begin{pmatrix} u_k^{(\pm)}(t=0) \\ v_k^{(\pm)}(t=0) \end{pmatrix} = \begin{pmatrix} \sin \frac{k}{2} \\ \cos \frac{k}{2} \end{pmatrix}. \quad (79)$$

We are now facing the problem of calculating the expectation value of the longitudinal magnetization

$$M_{x/y}(t) = \langle \psi^{(r)}(t) | \sum_{j=1}^N \sigma_j^{x/y} | \psi^{(r)}(t) \rangle, \quad (80)$$

which seems challenging at first sight because the state $|\psi^{(r)}(t)\rangle$ is a momentum-space state containing components with both fermion parities, while $\sum_{j=1}^N \sigma_j^{x/y}$ are written in the real-space and, more importantly, they break the fermion parity.

Thanks to the translational invariance of the initial state $|\psi_{g=0}^{(r)}\rangle$ and the driving Hamiltonian $H^{(\text{driv})}$, the expectation values of each $\sigma_j^{x/y}$ should be independent of j and we need only to calculate, for example, the boundary magnetization $\sigma_1^{x/y}$. We thus have

$$M_x(t) = N \langle \psi^{(r)}(t) | (c_1 + c_1^\dagger) | \psi^{(r)}(t) \rangle,$$

$$M_y(t) = N \langle \psi^{(r)}(t) | i(c_1 - c_1^\dagger) | \psi^{(r)}(t) \rangle, \quad (81)$$

as $\sigma_1^{x/y}$ can be written in terms of the Jordan-Wigner fermions as $\sigma_1^x = c_1 + c_1^\dagger$ and $\sigma_1^y = i(c_1 - c_1^\dagger)$. To proceed, we write c_1 in the momentum space as

$$\begin{aligned} c_1 &= P_+ c_1 P_- + P_- c_1 P_+ \\ &= \sum_{\sigma=\pm} P_{-\sigma} \frac{e^{i\pi/4}}{\sqrt{N}} \sum_{k \in K_\sigma} e^{ik} c_{k\sigma} P_\sigma. \end{aligned} \quad (82)$$

From the above equation and the explicit form of $|\psi^{(r)}(t)\rangle$ given by Eq. (77), we obtain after a straightforward, but lengthy calculation

$$\begin{aligned} &\langle \psi^{(r)}(t) | c_1 | \psi^{(r)}(t) \rangle \\ &= \frac{1}{2\sqrt{N}} e^{-i\gamma(t)} \left(\prod_{p>0, p \in K_+} +\langle X_p | \right) \left(\prod_{k>0, k \in K_-} |X_k\rangle_- \right) \\ &\quad + \frac{1}{2\sqrt{N}} e^{-i\gamma(t)} \left(\prod_{p>0, p \in K_+} +\langle X_p | \right) \left(\sum_{k' \in K_-, k'>0} v_{k'}^{(-)} (e^{ik'} | -k'\rangle_- - e^{-ik'} |k'\rangle_-) |k=0\rangle \prod_{k>0, k \in K_-, k(\neq k')} |X_k\rangle_- \right) \\ &\quad + \frac{i}{2\sqrt{N}} e^{i\gamma(t)} \left(\langle k=0 | \prod_{k>0, k \in K_-} -\langle X_k | \right) \left(\sum_{p' \in K_+, p'>0} v_{p'}^{(+)} [e^{ip'} | -p'\rangle_+ - e^{-ip'} |p'\rangle_+] \prod_{p>0, p \in K_+, p(\neq p')} |X_p\rangle_+ \right) \end{aligned} \quad (83)$$

where we have defined

$$\begin{aligned} \gamma(t) &\equiv \frac{1}{2} \int_0^t ds [h_1^{(-\pi)}(s) + h_2^{(0)}(s)], \\ |X_k\rangle_\pm &\equiv [u_k^{(\pm)} + v_k^{(\pm)} c_{k,\pm}^\dagger c_{-k,\pm}^\dagger] |0\rangle_{k,\pm}. \end{aligned} \quad (84)$$

Even though we can obtain the mode state $|X_k\rangle_\pm$ by solving (78), we are forced to evaluate the inner products between two product states with *distinct* fermion parities appearing in Eq. (83). In general, we have to calculate

$$I_{m,n} = \prod_{l=1, p_l>0, p_l \in K_\sigma}^m \sigma \langle X_{p_l} | \prod_{j=1, k_j>0, k_j \in K_{\bar{\sigma}}}^n |X_{k_j}\rangle_{\bar{\sigma}}. \quad (85)$$

We now use the following trick to write $|X_k\rangle_\pm$ as

$$|X_k\rangle_\pm = \frac{1}{v_k^{(\pm)}} \xi_{k,\pm}^\dagger \eta_{k,\pm}^\dagger |0\rangle_{k,\pm}, \quad (86)$$

where

$$\begin{aligned} \xi_{k,\pm}^\dagger &\equiv u_k^{(\pm)} c_{k,\pm} - v_k^{(\pm)} c_{-k,\pm}^\dagger, \\ \eta_{k,\pm}^\dagger &\equiv u_k^{(\pm)} c_{-k,\pm} + v_k^{(\pm)} c_{k,\pm}^\dagger, \end{aligned} \quad (87)$$

are two time-dependent effective Bogoliubov fermions which satisfy the usual anticommutation relations of fermions. So $I_{m,n}$ can be expressed as the vacuum expectation value of a product of $2(m+n)$ Bogoliubov fermions:

$$I_{m,n} = \frac{(-1)^m}{\prod_{l=1}^m v_{p_l}^{(\sigma)*} \prod_{j=1}^n v_{k_j}^{(\bar{\sigma})}} \langle 0 | \prod_{l=1, p_l>0, p_l \in K_\sigma}^m \xi_{p_l, \sigma} \eta_{p_l, \sigma} \prod_{j=1, k_j>0, k_j \in K_{\bar{\sigma}}}^n \xi_{k_j, \bar{\sigma}}^\dagger \eta_{k_j, \bar{\sigma}}^\dagger | 0 \rangle. \quad (88)$$

Now we can use Wick's theorem to write the above expectation value as the Pfaffian of a $2(m+n) \times 2(m+n)$ antisymmetric matrix $A^{(m,n)}$

$$I_{m,n} = \frac{(-1)^m}{\prod_{l=1}^m v_{p_l}^{(\sigma)*} \prod_{j=1}^n v_{k_j}^{(\bar{\sigma})}} \text{Pf} A^{(m,n)}. \quad (89)$$

To find out the nonvanishing entries of $A^{(m,n)}$, we note that there are six types of nonvanishing contractions:

$$\begin{aligned}
\langle 0 | \xi_{p_l, \sigma} \eta_{p_l, \sigma} | 0 \rangle &= -u_{p_l}^{(\sigma)*} v_{p_l}^{(\sigma)*}, \\
\langle 0 | \xi_{k_j, \bar{\sigma}}^\dagger \eta_{k_j, \bar{\sigma}}^\dagger | 0 \rangle &= u_{k_j}^{(\bar{\sigma})} v_{k_j}^{(\bar{\sigma})}, \\
\langle 0 | \xi_{p_l, \sigma} \xi_{k_j, \bar{\sigma}}^\dagger | 0 \rangle &= v_{p_l}^{(\sigma)*} v_{k_j}^{(\bar{\sigma})} f_{-p_l, -k_j}, \\
\langle 0 | \xi_{p_l, \sigma} \eta_{k_j, \bar{\sigma}}^\dagger | 0 \rangle &= -v_{p_l}^{(\sigma)*} v_{k_j}^{(\bar{\sigma})} f_{-p_l, k_j}, \\
\langle 0 | \eta_{p_l, \sigma} \xi_{k_j, \bar{\sigma}}^\dagger | 0 \rangle &= -v_{p_l}^{(\sigma)*} v_{k_j}^{(\bar{\sigma})} f_{p_l, -k_j}, \\
\langle 0 | \eta_{p_l, \sigma} \eta_{k_j, \bar{\sigma}}^\dagger | 0 \rangle &= v_{p_l}^{(\sigma)*} v_{k_j}^{(\bar{\sigma})} f_{p_l, k_j},
\end{aligned} \tag{90}$$

which give the following nonvanishing entries (for $l = 1, 2, \dots, m$ and $j = 1, 2, \dots, n$)

$$\begin{aligned}
A_{2l-1, 2l}^{(m,n)} &= -u_{p_l}^{(\sigma)*} v_{p_l}^{(\sigma)*}, \\
A_{2m+2j-1, 2m+2j}^{(m,n)} &= u_{k_j}^{(\bar{\sigma})} v_{k_j}^{(\bar{\sigma})}, \\
A_{2l-1, 2m+2j-1}^{(m,n)} &= v_{p_l}^{(\sigma)*} v_{k_j}^{(\bar{\sigma})} f_{-p_l, -k_j}, \\
A_{2l-1, 2m+2j}^{(m,n)} &= -v_{p_l}^{(\sigma)*} v_{k_j}^{(\bar{\sigma})} f_{-p_l, k_j}, \\
A_{2l, 2m+2j-1}^{(m,n)} &= -v_{p_l}^{(\sigma)*} v_{k_j}^{(\bar{\sigma})} f_{p_l, -k_j}, \\
A_{2l, 2m+2j}^{(m,n)} &= v_{p_l}^{(\sigma)*} v_{k_j}^{(\bar{\sigma})} f_{p_l, k_j}.
\end{aligned} \tag{91}$$

The matrix element $A_{i,j}^{(m,n)}$ with $i > j$ can be obtained from the relation $A_{i,j}^{(m,n)} = -A_{j,i}^{(m,n)}$.

Fortunately, the efficient numerical computation of the Pfaffian of $A^{(m,n)}$ can be managed by using the software package presented in [27]. Thus, $M_{x/y}(t)$ can be numerically calculated by combining Eqs. (81), (83), and (89). The dynamics of the transverse magnetization $M_z(t) = \langle \psi^{(r)}(t) | \sum_{j=1}^N \sigma_j^z | \psi^{(r)}(t) \rangle$ can be calculated by noting that

$$\begin{aligned}
\sum_i \sigma_i^z &= 2 \sum_{k>0, k \in K_+} [|k, -k\rangle_+ + \langle k, -k| - |0\rangle_{k,+} \langle k, +\langle 0|] \\
&+ 2 \sum_{k>0, k \in K_-} [|k, -k\rangle_- - \langle k, -k| - |0\rangle_{k,-} \langle k, -\langle 0|] \\
&+ [|k = -\pi\rangle_- - \langle k = -\pi| - |0\rangle_{-\pi,-} \langle -\pi, -\langle 0|] \\
&+ [|k = 0\rangle_- - \langle k = 0| - |0\rangle_{0,-} \langle 0, -\langle 0|].
\end{aligned} \tag{92}$$

Since $\sum_i \sigma_i^z$ preserves the fermion parity, $M_z(t)$ can be easily calculated as

$$\begin{aligned}
M_z(t) &= \sum_{k>0, k \in K_+} [|v_k^{(+)}(t)|^2 - |u_k^{(+)}(t)|^2] \\
&+ \sum_{k>0, k \in K_-} [|v_k^{(-)}(t)|^2 - |u_k^{(-)}(t)|^2].
\end{aligned} \tag{93}$$

In the next subsection we will discuss several examples for which the procedure developed in this subsection can be applicable.

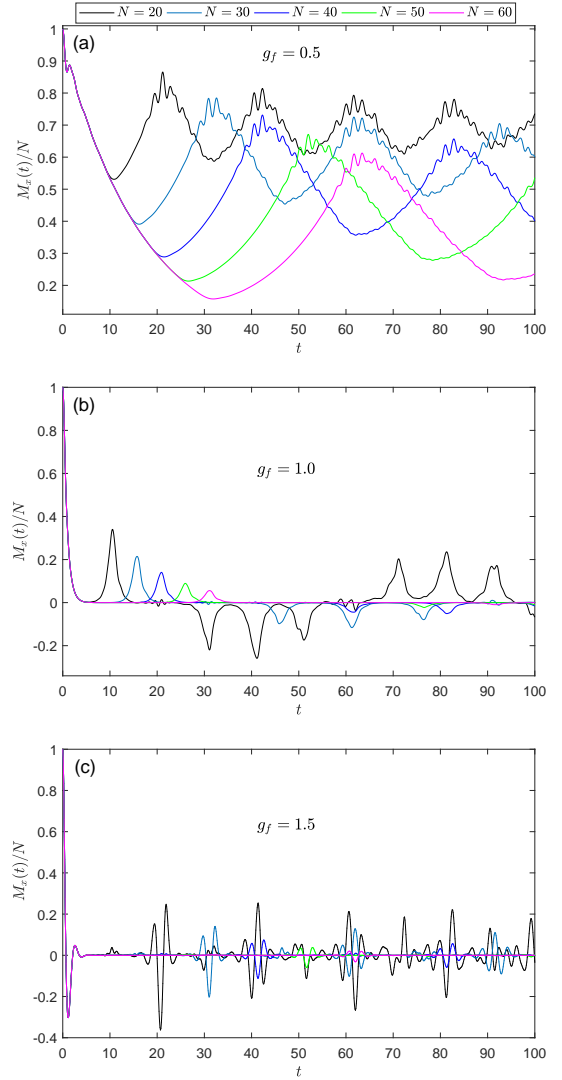


FIG. 3: Dynamics of the longitudinal magnetization $M_x(t)/N$ after a sudden quench of the magnetic field from $g_i = 0$ to g_f . (a) $g_f = 0.5$, (b) $g_f = 1.0$, (c) $g_f = 1.5$. The initial state is prepared as the ferromagnetic state $|\psi_{g=0}^{(r)}\rangle = |\rightarrow\rangle_1 \cdots |\rightarrow\rangle_N$.

B. Numerical examples

1. Sudden quench

Our first example is the time evolution governed by the Hamiltonian of the quantum Ising ring with finite magnetic field g . This process can be viewed as a sudden quench of the parameter g from the initial value $g_i = 0$ to the final value $g_f > 0$. In this case the driving Hamiltonian is consistent with Eq. (22), i.e., $\mathcal{H}_{k,\sigma}^{(\text{driv})} = \mathcal{H}_{k,\sigma}^{(e)}$ and $\gamma(t) = \frac{1}{2} \int_0^t ds [-2(1-g) - 2(1+g)] = -2t$.

Figure 3(a) shows the evolution of $M_x(t)/N$ for a sudden quench to $g_f = 0.5$, which occurs within the ordered phase. It can be seen that $M_x(t)/N$ experiences a universal decay that is almost independent of the system size

N at short-times scales. At a time around $t_{\min} \approx N/2$, $M_x(t)/N$ reaches its first minimum $M_x^{(\min)}(t)/N$ that decreases with increasing N . Numerical fittings approximately give $t_{\min} = 0.525N + 0.4$ and $M_x^{(\min)}(t)/N = 0.9744e^{-0.0304N}$, showing that $M_x^{(\min)}(t)/N$ decreases exponentially with increasing N . After that, $M_x(t)/N$ exhibits a quasi-periodic oscillatory behavior with period $T \approx N$. It is expected that $M_x(t)/N$ decays exponentially in the thermodynamics limit and approaches zero in the long-time limit. These observations are qualitatively consistent with previous works which deal with quenches within the ordered phase in either infinite systems [28] or for open boundary conditions [29, 30].

Figure 3(b) shows the dynamics of $M_x(t)/N$ for a sudden quench to the critical point $g_f = 1.0$. A universal but abrupt short-time decay to nearly zero is observed. In contrast to the quench within the critical phase, $M_x(t)/N$ reaches its first maximum around $t_{\max} \approx N/2$. These maxima decrease exponentially with increasing N . Numerical fittings approximately give $t_{\max} = 0.515N + 0.24$ and $M_x^{(\max)}(t)/N = 0.8316e^{-0.04478N}$. For large enough chains, $M_x(t)/N$ almost collapses after the initial decay process.

Figure 3(c) shows the dynamics of $M_x(t)/N$ for a sudden quench to the disordered phase with $g_f = 1.5$. We observe more abrupt short-time decay of $M_x(t)/N$ to negative values, but followed by a sharp increase to nearly zero. After that $M_x(t)/N$ tends to collapse but exhibits minor revivals at around $t \approx N$.

2. delta kick

Following Ref. [13], we study the following protocol. Suppose we start with $|\psi(0)\rangle = |\psi_{g=0}^{(r)}\rangle$ and evolve the system with H_{QIM} for a time τ . Then we apply a delta kick

$$K_\phi = e^{-i\frac{\phi}{2} \sum_i \sigma_i^z}, \quad (94)$$

which rotates the spins about the z axis by an angle

$$\phi = \pi(1 - \epsilon), \quad (95)$$

where ϵ is a perturbation. The time evolution over one period is

$$U(\tau) = K_{\pi(1-\epsilon)} e^{-iH_{\text{QIM}}\tau}. \quad (96)$$

The state of system just after the n th kick is

$$\begin{aligned} |\psi(n)\rangle &= U^n |\psi(0)\rangle \\ &= K_{\pi(1-\epsilon)} e^{-iH_{\text{QIM}}\tau} \dots K_{\pi(1-\epsilon)} e^{-iH_{\text{QIM}}\tau} |\psi_{g=0}^{(r)}\rangle. \end{aligned} \quad (97)$$

For $\epsilon = 0$ and $g = 0$, the initial state is an eigenstate of $H_{\text{QIM}}(g = 0)$, so that the spins flip at $n\tau$ and the system returns to the initial state at every 2τ .

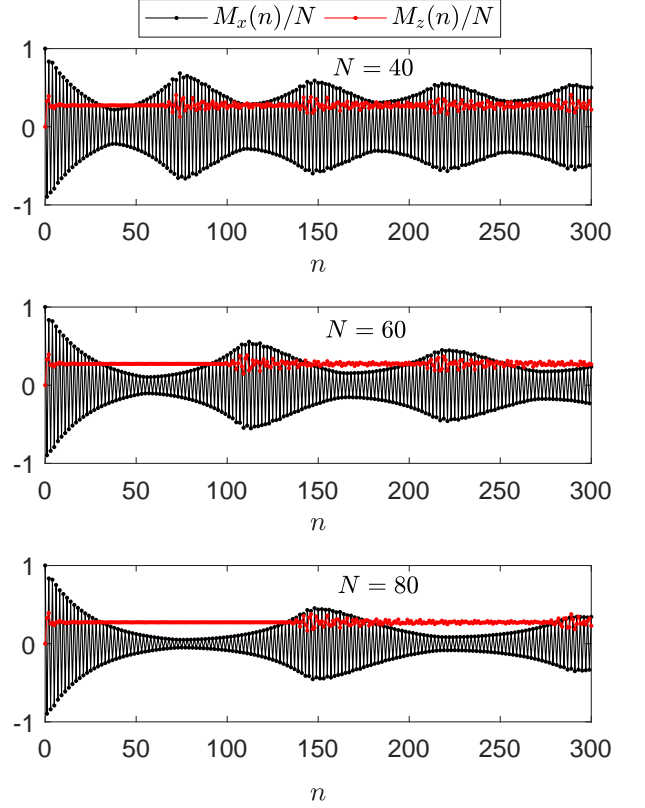


FIG. 4: Stroboscopic longitudinal magnetization $M_x(n)/N$ and transverse magnetization $M_z(n)/N$ as functions of number of kicks n for various system sizes N . The initial state is prepared as the ferromagnetic state $|\psi_{g=0}^{(r)}\rangle = |\rightarrow\rangle_1 \dots |\rightarrow\rangle_N$. Parameters: $g = 0.5$, $\tau = 0.5$, and $\epsilon = 0.02$.

Note that both H_{QIM} and K_ϕ conserve the parity of the fermions and are translationally invariant, so we can write

$$\begin{aligned} e^{-iH_{\text{QIM}}\tau} &= P_+ \prod_{k>0, k \in K_+} e^{-i\mathcal{H}_{k,+}^{(e)}\tau} P_+ \\ &+ P_- e^{-\frac{1}{2}i\mathcal{H}_{-,\pi,-}\tau} e^{-\frac{1}{2}i\mathcal{H}_{0,-}\tau} \prod_{k>0, k \in K_-} e^{-i\mathcal{H}_{k,-}^{(e)}\tau} P_- \end{aligned} \quad (98)$$

and

$$\begin{aligned} K_\phi &= P_- e^{-i\frac{\phi}{2}\mathcal{F}_{-,\pi,-}} e^{-i\frac{\phi}{2}\mathcal{F}_{0,-}} \prod_{k>0, k \in K_-} e^{-i\frac{\phi}{2}\mathcal{F}_{k,-}} P_- \\ &+ P_+ \prod_{k>0, k \in K_+} e^{-i\frac{\phi}{2}\mathcal{F}_{k,+}} P_+, \end{aligned} \quad (99)$$

where

$$\begin{aligned} \mathcal{F}_{k,\sigma} &= 2 \begin{pmatrix} -1 & 0 \\ 0 & 1 \end{pmatrix}, \\ \mathcal{F}_{-,\pi,-} &= \begin{pmatrix} -1 & 0 \\ 0 & 1 \end{pmatrix}, \quad \mathcal{F}_{0,-} = \begin{pmatrix} -1 & 0 \\ 0 & 1 \end{pmatrix}. \end{aligned} \quad (100)$$

We have used Eq. (92) in deriving Eq. (99). Hence,

$$\begin{aligned}
U^n = & P_+ \prod_{k>0, k \in K_+} (e^{-i\frac{\phi}{2}\mathcal{F}_{k,+}} e^{-i\mathcal{H}_{k,+}^{(e)}\tau})^n P_+ \\
& + P_- (e^{-i\frac{\phi}{2}\mathcal{F}_{-\pi,-}} e^{-\frac{1}{2}i\mathcal{H}_{-\pi,-}\tau})^n (e^{-i\frac{\phi}{2}\mathcal{F}_{0,-}} e^{-\frac{1}{2}i\mathcal{H}_{0,-}\tau})^n \\
& \prod_{k>0, k \in K_-} (e^{-i\frac{\phi}{2}\mathcal{F}_{k,-}} e^{-i\mathcal{H}_{k,-}^{(e)}\tau})^n P_-. \quad (101)
\end{aligned}$$

When acting on the initial state, we finally get

$$\begin{aligned}
|\psi(n)\rangle = & \frac{1}{\sqrt{2}} \prod_{k>0, k \in K_+} (e^{-i\frac{\phi}{2}\mathcal{F}_{k,+}} e^{-i\mathcal{H}_{k,+}^{(e)}\tau})^n \chi_{k,+} \\
& + \frac{e^{-i\frac{\pi}{4}}}{\sqrt{2}} e^{i2n\tau} \chi_{-\pi,-} \chi_{0,-} \prod_{k>0, k \in K_-} (e^{-i\frac{\phi}{2}\mathcal{F}_{k,-}} e^{-i\mathcal{H}_{k,-}^{(e)}\tau})^n \chi_{k,-}, \quad (102)
\end{aligned}$$

where

$$\chi_{k,\sigma} = \begin{pmatrix} \sin \frac{k}{2} \\ \cos \frac{k}{2} \end{pmatrix}, \quad \chi_{-\pi,-} = \begin{pmatrix} 1 \\ 0 \end{pmatrix}, \quad \chi_{0,-} = \begin{pmatrix} 0 \\ 1 \end{pmatrix}. \quad (103)$$

The evolution of $M_x(t)$ can now be calculated by using the Pfaffian method presented in Sec. IV A. In Fig. 4 we show both the stroboscopic longitudinal magnetization $M_x(t)/N$ and transverse magnetization $M_z(t)/N$ as functions of the number of kicks n for different system sizes. It can be seen that $M_x(t)/N$ breaks the time-translational symmetry but shows a persistent oscillatory profile with a fixed period approximately proportional to N . While the transverse magnetization $M_z(t)/N$ only experiences small oscillators when $M_x(t)/N$ showing peaks.

The numerical simulations performed are far beyond the reach of exact diagonalization used in Ref. [13]. Our formalism thus provides a numerically efficient way to study the emergence of discrete time crystals in the quantum Ising setup with finite but large number of spins.

V. CONCLUSIONS AND DISCUSSIONS

In this work, we revisit several aspects of the finite-size quantum Ising chain with periodic boundary con-

ditions. In special, we show that the momentum-space BCS-type ground states of the classical Ising ring are proportional to the equally-weighted linear superpositions of the two fully aligned ferromagnetic states. This relationship is a special case of the correspondence between the spatially factorized ground states of the XYZ spin chain under frustration-free conditions and the two fermionic states with distinct fermion parities in the Jordan-Wigner fermion representation.

Based on the above relationship between the real-space and momentum-space representations of the same state, we study the real-time dynamics of the longitudinal magnetization $\sum_i \sigma_i^x$ under translationally invariant driving Hamiltonians, with the system prepared in one of the ferromagnetic states. Since the ferromagnetic state is a linear superposition of states with distinct fermion parities, the calculation of the parity-breaking longitudinal magnetization dynamics is less straightforward. Fortunately, by writing the BCS mode state as the occupation state of two time-dependent effective Bogoliubov fermions, we are able to derive a Pfaffian formula for the calculation of the longitudinal magnetization dynamics. The obtained formalism is then applied to two dynamical scenarios, namely the sudden quench and delta kicks. With the help of software package that can realize efficient numerical computation of Pfaffians, we perform numerical simulations for both scenarios in relatively large systems.

Note added: While the present manuscript was nearly finished, we became aware of a related preprint [31] in which the authors also studied the dynamics of the longitudinal magnetization starting with a ferromagnetic state. Though there is certain amount of overlap between the two works, we note that in Ref. [31] the dynamics of the longitudinal magnetization in a periodic chain, which is the main focus of our work, is calculated for at most $N = 12$ spins using exact diagonalization.

Acknowledgements: We thank Hosho Katsura for useful discussion on the Perron-Frobenius theorem. We also thank W.-L. You for bringing Ref. [13] to our attention. This work was supported by the NSFC under Grant Numbers 11705007, and partially by the Beijing Institute of Technology Research Fund Program for Young Scholars.

-
- [1] S. Sachdev, *Quantum phase transitions* (Cambridge University Press, Cambridge, 1999).
 - [2] T. J. Osborne and M. A. Nielsen, Phys. Rev. A **66**, 032110 (2002).
 - [3] A. Osterloh, L. Amico, G. Falci, and R. Fazio, Nature (London) **416**, 608 (2002).
 - [4] G. Vidal, J. I. Latorre, E. Rico, and A. Kitaev, Phys. Rev. Lett. **90**, 227902 (2003).
 - [5] Z. Chang and N. Wu, Phys. Rev. A **81**, 022312 (2010).

- [6] W. H. Zurek, U. Dorner, and P. Zoller, Phys. Rev. Lett. **95**, 105701 (2005).
- [7] J. Dziarmaga, Phys. Rev. Lett. **95**, 245701 (2005).
- [8] H. T. Quan, Z. Song, X. F. Liu, P. Zanardi, and C. P. Sun, Phys. Rev. Lett. **96**, 140604 (2006).
- [9] A. del Campo, M. M. Rams, and W. H. Zurek, Phys. Rev. Lett. **109**, 115703 (2012).
- [10] N. Wu, A. Nanduri, and H. Rabitz, Phys. Rev. B **91**, 041115(R) (2015).

- [11] M. Heyl, A. Polkovnikov, and S. Kehrein, *Phys. Rev. Lett.* **110**, 135704 (2013).
- [12] P. Titum, J. T. Iosue, J. R. Garrison, A. V. Gorshkov, and Z.-X. Gong, *Phys. Rev. Lett.* **123**, 115701 (2019).
- [13] W. C. Yu, J. Tangpanitanon, A. W. Glaetzle, D. Jaksch, and D. G. Angelakis, *Phys. Rev. A* **99**, 033618 (2019).
- [14] E. Lieb, T. Schultz, and D. Mattis, *Ann. Phys. (NY)* **16**, 407 (1961).
- [15] G. G. Cabrera and R. Jullien, *Phys. Rev. B* **35**, 7062 (1987).
- [16] A. De Pasquale and P. Facchi, *Phys. Rev. A* **80**, 032102 (2009).
- [17] A. F. Albuquerque, F. Alert, C. Sire, and S. Capponi, *Phys. Rev. B* **81**, 064418 (2010).
- [18] H. Katsura, *J. Phys. A: Math. Theor.* **45**, 115003 (2012).
- [19] B. Damski and M. M. Rams, *J. Phys. A: Math. Theor.* **47**, 025303 (2014).
- [20] M. Okuyama, Y. Yamanaka, H. Nishimori, and M. M. Rams, *Phys. Rev. E* **92**, 052116 (2015).
- [21] A. Yu. Kitaev, *Phys. Usp.* **44**, 131 (2001).
- [22] P. Fendley, *J. Phys. A: Math. Theor.* **49**, 30LT01 (2016).
- [23] M. Greiter, V. Schnells, and R. Thomale, *Ann. Phys. (NY)* **351**, 1026 (2014).
- [24] J. Kurmann, H. Thomas, and G. Müller, *Physica A* **112**, 235 (1982).
- [25] H. Katsura, D. Schuricht, and M. Takahashi, *Phys. Rev. B* **92**, 115137 (2015).
- [26] K. Kawabata, R. Kobayashi, N. Wu, and H. Katsura, *Phys. Rev. B* **95**, 195140 (2017).
- [27] M. Wimmer, *ACM Trans. Math. Softw.* **38**, 1 (2012).
- [28] P. Calabrese, F. H. L. Essler, and M. Fagotti, *Phys. Rev. Lett.* **106**, 227203 (2011).
- [29] F. Iglói and H. Rieger, *Phys. Rev. Lett.* **106**, 035701 (2011).
- [30] H. Rieger and F. Iglói, *Phys. Rev. B* **84**, 165117 (2011).
- [31] M. Białończyk and B. Damski, *arXiv: 1909.12853* (2019).